

# Dry and Wet Deposition of Nitrogen Emitted in Buenos Aires City to Waters of de la Plata River

Andrea L. Pineda Rojas · Laura E. Venegas

Received: 19 December 2007 / Accepted: 10 March 2008 / Published online: 3 April 2008  
© Springer Science + Business Media B.V. 2008

**Abstract** Dry and wet deposition of atmospheric nitrogen species ( $\text{NO}_2$  and  $\text{HNO}_3$ ) coming from nitrogen oxides emissions in Buenos Aires city to surface waters of de la Plata River were estimated. Atmospheric dispersion models DAUMOD-RD (v.2) and CALPUFF were applied to area and point sources, respectively. These models were run considering 1 year of hourly meteorological data. Emission information included a typical diurnal variation of area source emissions. Annual atmospheric nitrogen ( $\text{N-NO}_2 + \text{N-HNO}_3$ ) deposition to  $1,763 \text{ km}^2$  of the river was  $35,600 \text{ kg-N year}^{-1}$ . Dry deposition processes accounted for 89% of this value. The small contribution of wet deposition was a consequence of the very few cases (5%) of rain events during offshore wind conditions. Monthly dry deposition to  $1,763 \text{ km}^2$  of the river varied from  $1,628 \text{ kg-N month}^{-1}$  in February to  $3,799 \text{ kg-N month}^{-1}$  in December, following the monthly occurrence of

offshore winds. Monthly wet deposition varied from  $1 \text{ kg-N month}^{-1}$  in June to  $1,162 \text{ kg-N month}^{-1}$  in February. These results came from the combination of favorable conditions for formation of  $\text{HNO}_3$  and the occurrence of precipitation during offshore wind situations. Spatial distribution of annual atmospheric N deposition showed a strong coastal gradient. Deposition values reached a maximum of  $137.1 \text{ kg-N km}^{-2} \text{ year}^{-1}$  near the shoreline, which was reduced to the half at 4 km from the coast.

**Keywords** Atmospheric dispersion modeling · Buenos Aires · Dry deposition · Nitric acid · Nitrogen dioxide · Wet deposition

## 1 Introduction

In estuaries and coastal areas, nitrogen supplies to coastal waters have been considerably increased by human activities. Excessive inputs of nutrients to the aquatic system may cause eutrophication, which is considered a form of pollution because it promotes excessive plant growth with its consequent ecosystem degradation. In addition, where eutrophic conditions interfere with drinking water treatment, health-related problems may occur (Bartram et al. 1999). Hence, a proper determination of the nitrogen inputs is crucial to assess and understand the human activities impact on the aquatic system.

---

A. L. Pineda Rojas (✉) · L. E. Venegas  
Department of Atmospheric and Oceanic Sciences,  
Faculty of Sciences, University of Buenos Aires,  
National Scientific and Technological Research  
Council (CONICET),  
Ciudad Universitaria, Pab. 2,  
1428 Buenos Aires, Argentina  
e-mail: pineda@at.fcen.uba.ar

L. E. Venegas  
e-mail: venegas@at.fcen.uba.ar

Fixed nitrogen may reach an estuary via tributaries, overland runoff and flooding, subsurface water flow, discharge from storm water systems, industrial and sewage treatment plants, and by atmospheric deposition (Poor et al. 2001). Between all these nitrogen input sources, more attention is increasingly being given to the atmospheric contribution. Significant amounts of nitrogen compounds coming from emission sources located on the ground can be transferred to the waters through the atmosphere (Jickells 2002; Pryor and Sørensen 2002). The transfer of atmospheric nitrogen to the water surface can occur through wet and dry deposition processes. Wet deposition refers to the natural processes by which material is scavenged by atmospheric hydrometeors and consequently deposits onto the earth's surface during precipitation. Dry deposition is the transport of gaseous and particulate species from the atmosphere onto surfaces in the absence of precipitation.

Several authors have estimated the deposition of atmospheric nitrogen (N) on coastal waters at different sites. Some of the recent studies include the evaluation of N deposition on coastal waters at Tampa Bay (USA; Poor et al. 2001), the Baltic Sea (Pryor et al. 2001), the North Sea (Hertel et al. 2002), Barnegat Bay (USA; Gao 2002), Long Island Sound (USA; Luo et al. 2002), Greenwood Lake (USA; Imboden et al. 2003), the Neuse River estuary (USA; Whitall et al. 2003), the Seine River estuary (Garban et al. 2004) and the Kattegat Strait (Denmark; Carstensen et al. 2005).

De la Plata River is a shallow river-type estuary of 36,000 km<sup>2</sup> (see Fig. 1). On its southeast coast lies the city of Buenos Aires with an extension of 203 km<sup>2</sup> and 2,776,138 inhabitants. Near Buenos Aires city, the estuary is a freshwater turbid river-dominated environment with depths varying between 3–6 m. The estuary constitutes the main source of drinking water reservoir for the city and surrounding areas. Nagy et al. (2002) analyzed symptoms of eutrophication in the estuary and determined that the system is moderately eutrophied. Nevertheless, according to these authors, increasing trends in quantity of freshwater and nutrient loads, and the low potential to dilute and flush nutrients, suggest that the estuary is prone to worsening eutrophication conditions like oxygen stress and harmful blooms. Some authors have estimated nitrogen inputs from the main tributaries

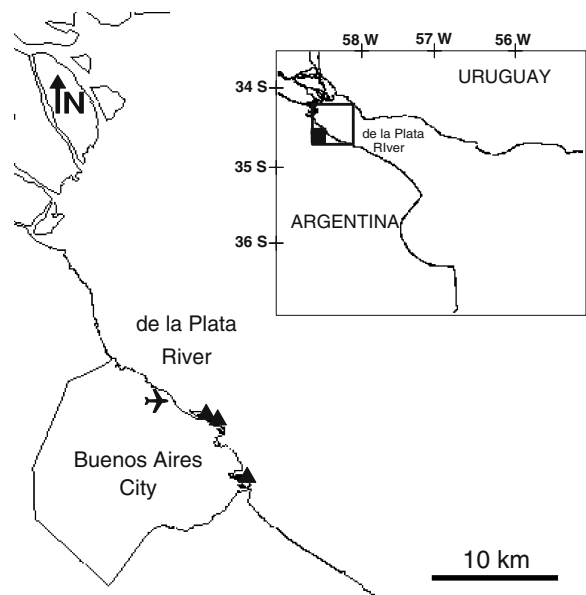


**Fig. 1** Buenos Aires City and the coastal waters (1,763 km<sup>2</sup>) of the de la Plata River. The *little map* shows the geographic location of the study area. (✈ Domestic airport,  $\blacktriangle$  power plant)

and sewage discharges from Buenos Aires city (Pizarro and Orlando 1985; Nagy 2000); however, little attention has been previously given to the atmospheric contribution. A recent study (Pineda Rojas and Venegas 2008) reports a first estimation of two atmospheric nitrogen compounds deposited to waters of de la Plata River. In this previous work, only dry deposition of nitrogen dioxide (NO<sub>2</sub>) and nitric acid (HNO<sub>3</sub>) has been estimated applying the DAUMOD-RD (v.1) model to area source emissions of nitrogen oxides (NO<sub>x</sub>) and CALPUFF (Scire et al. 2000) model to point sources, located in the city of Buenos Aires.

The aim of this study is to estimate wet and dry deposition of N–NO<sub>2</sub> and N–HNO<sub>3</sub> to waters of de la Plata River, considering the NO<sub>x</sub> emitted in the city of Buenos Aires. In order to achieve this task we have developed DAUMOD-RD (v.2) which includes parameterisations of both dry and wet deposition processes. DAUMOD-RD (v.2) is applied to area source emissions and CALPUFF model to point source emissions. Estimations of wet and dry deposition of N–NO<sub>2</sub> and N–HNO<sub>3</sub> are presented, the relative importance of each of these processes on total deposition of nitrogen is analyzed, and the main

factors controlling the deposition of atmospheric N to de la Plata River are discussed.

## 2 Nitrogen Oxides Emitted in the City of Buenos Aires

The atmospheric pollutants of interest in this work are NO<sub>2</sub> and HNO<sub>3</sub> generated from NO<sub>x</sub> emitted from sources located in Buenos Aires city.

Main sources of NO<sub>x</sub> located in the city can be grouped into area and point sources, following an emission inventory recently developed (Mazzeo and Venegas 2003). This inventory includes as area sources the emissions from domestic, commercial and small industry activities; road traffic (buses, cars/taxis and trucks); and emissions at the Domestic Airport located in Buenos Aires city (see Fig. 1). The emissions inventory of NO<sub>x</sub> (expressed as NO<sub>2</sub>) for area sources has a spatial resolution of 1 km<sup>2</sup> over the city. A typical diurnal variation is also provided, showing higher emission values at 8:00 A.M. and at (7:00–8:00) P.M. and lower emissions at night. Point sources are the 14 stacks of three thermal power plants located on the coast (see Fig. 1). Since there are no other large industries within the city, the stacks of the power plants are the only point sources to be considered.

The estimated total annual emission of NO<sub>x</sub> (expressed as NO<sub>2</sub>) is 53,961 ton year<sup>-1</sup> (Mazzeo and Venegas 2003). Relative contribution of each source category to total NO<sub>x</sub> annual emission in the city is shown in Fig. 2. It can be seen that 45.6% of

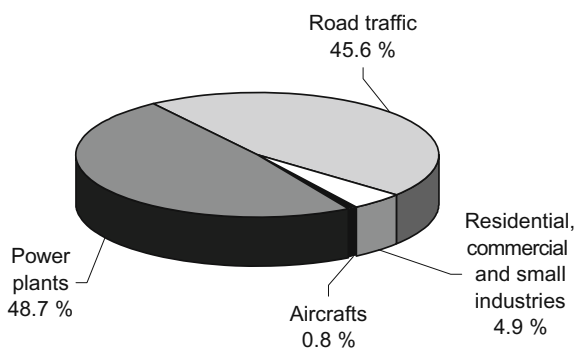


**Fig. 2** Relative contributions of each source category to total NO<sub>x</sub> emission in Buenos Aires city. (Source: Mazzeo and Venegas 2003)

annual NO<sub>x</sub> emissions within the city can be allocated to road traffic and 48.7% to thermal power plants.

## 3 Atmospheric Dispersion–Deposition Models Used in Calculations

### 3.1 DAUMOD-RD (v.2) Model

The DAUMOD-RD (v.2) model is a recent version of the initial DAUMOD atmospheric dispersion model (Mazzeo and Venegas 1991). It is an atmospheric dispersion model applicable to area sources distributed in urban areas. DAUMOD model is based on the semi-empirical bi-dimensional equation of dispersion, but neither removal processes of pollutants from the atmosphere nor chemical reactions are included in it. Former DAUMOD model has been satisfactory evaluated in different cities of Europe and the USA, as well as in the city of Buenos Aires (Mazzeo and Venegas 1991, 2004; Venegas and Mazzeo 2002, 2006).

In an urban area, a horizontal distribution of area sources with strength varying according to a typical square grid pattern may be assumed. Each grid cell is a continuously emitting area source of uniform strength  $Q_i$  ( $i=0, 1, 2, \dots, N$ ). According to DAUMOD (and also DAUMOD-RD), the variation of air pollutant concentration ( $C$ ) with distance ( $x$ ) in the direction of the mean wind and height ( $z$ ) is given by:

$$C(x,z) = \frac{a \left[ Q_0 x^b + \sum_{i=1}^N (Q_i - Q_{i-1})(x - x_i)^b \right]}{|A_1| k z_0^b u_*} \times \sum_{j=0}^6 A_j \left( \frac{z}{h} \right)^j \tag{1}$$

where  $N$  is the number of sources upwind the receptor,  $u_*$  is the friction velocity,  $k$  is the von Karman constant ( $=0.41$ ),  $z_0$  is the surface roughness length, coefficients  $a$ ,  $b$  and  $A_j$  are functions of the atmospheric stability ( $z_0/L$ ), being  $L$  the Monin-Obukhov length and  $h$  is the vertical extension of

the plume of contaminants. The variation of  $h$  with distance is given by (Mazzeo and Venegas 1991):

$$h(x) = a \left( \frac{x}{z_0} \right)^b z_0 \tag{2}$$

The expressions of  $a$ ,  $b$  and  $A_j$  are included in Tables 1 and 2.

The DAUMOD-RD (v.2) model incorporates a chemical transformation scheme to evaluate NO<sub>2</sub> and HNO<sub>3</sub> surface concentrations and parameterization of deposition processes of these species over a water surface, that are similar to the included in CALPUFF model (Scire et al. 2000). A complete description of the parameterizations incorporated in DAUMOD-RD to estimate formation of HNO<sub>3</sub> and dry deposition fluxes of NO<sub>2</sub> and HNO<sub>3</sub> can be found in Pineda Rojas and Venegas (2008). However, the main assumptions of those schemes are described next.

As a conservative approximation, in both models (CALPUFF and DAUMOD v.2) the NO<sub>x</sub> emitted is considered as nitrogen dioxide (NO<sub>2</sub>). Some fraction of NO<sub>2</sub> is removed from the atmosphere via the formation of nitric acid (HNO<sub>3</sub>) and organic nitrates (RNO<sub>3</sub>; Atkinson et al. 1982; Atkinson 2000; Khoder 2002) and the rest can be transferred to the water surface by dry deposition. According to the photochemical model developed by Scire et al. (1984, 2000), diurnal transformation rates for the NO<sub>2</sub> loss and the HNO<sub>3</sub> formation can be parameterized in terms of environmental conditions as follows:

$$k_1 = 1,206[\text{O}_3]^{1.5} S^{-1.41} [\text{NO}_x]_m^{-0.329} \tag{3}$$

**Table 1** Expressions of parameters  $a$  and  $b$  as functions of  $z_0/L$

Atmospheric stability	Expressions of $a$ and $b$
$z_0/L < -10^{-4}$	$a = 3.618833 + 0.2369076 \ln( z_0/L )$ $b = 0.5356147 + 0.0234187 \ln [( z_0/L ) + 0.01]$
$-10^{-4} \leq z_0/L \leq 10^{-4}$	$a = -384.73 (z_0/L) + 1.4$ $b = -130.0 (z_0/L) + 0.415$
$10^{-4} < z_0/L$	$a = 0.6224632 + 7.37387E-05/\ln [(z_0/L) + 1]$ $b = 0.5065736 - 1.196137/\ln [2,802.315 + 9/(z_0/L)]$

**Table 2** Expressions of parameters  $A_j$  as functions of  $z_0/L$

Atmospheric stability	Expressions of $A_j$
$z_0/L < -10^{-2}$	$A_j = A_j(z_0/L = -0.01)$
$-10^{-2} \leq z_0/L < -10^{-4}$	$A_0 = 1.0$ $A_1 = -9.254667 - 0.8043134 \ln( z_0/L )$ $A_2 = -26.88303107 - 197.989893 [\ln(1.2146  z_0/L )]^{-1}$ $A_3 = -38.00005 + \exp[4.16612 - 373.1065  z_0/L ]$ $A_4 = -84.48740174 - 333.915544 [\ln(7.5651  z_0/L )]^{-1}$ $A_5 = -33.25054 + \exp[4.13875 - 289.5308  z_0/L ]$ $A_6 = -14.47563571 - 43.4735075 [\ln(14.5776  z_0/L )]^{-1}$
$-10^{-4} \leq z_0/L \leq 10^{-4}$	$A_0 = 1.0$ $A_1 = 3,853.3 (z_0/L) - 1.461$ $A_2 = -18,740 (z_0/L) - 6.797$ $A_3 = 27,740 (z_0/L) + 26.931$ $A_4 = -16,270 (z_0/L) - 39.652$ $A_5 = 965 (z_0/L) + 27.781$ $A_6 = 1,635 (z_0/L) - 7.655$
$10^{-4} < z_0/L$	$A_0 = 1.0$ $A_1 = -0.05478233 - 0.0001021171 [\ln[(z_0/L) + 1]]^{-1}$ $A_2 = -6.55023478 + 0.02035983 [\ln(z_0/L)]^3 + 0.00191583 [\ln(z_0/L)]^4$ $A_3 = 12.9282233 + \exp[2.917612 - 1,007.8064 (z_0/L)]$ $A_4 = -0.59677391 + 0.05583574 [\ln(z_0/L)]^3 + 0.00040899 [\ln(z_0/L)]^4$ $A_5 = -1.9551195 + \exp[3.5211141 - 1,255.2843 (z_0/L)]$ $A_6 = 2.66883478 + 0.00810494 [\ln(z_0/L)]^3 - 0.00053199 [\ln(z_0/L)]^4$

$$k_2 = 1,262[\text{O}_3]^{1.45} S^{-1.34} [\text{NO}_x]_m^{-0.122} \tag{4}$$

where  $k_1$  is the NO<sub>x</sub> to (HNO<sub>3</sub>+RNO<sub>3</sub>) transformation rate (percent per hour),  $k_2$  is the NO<sub>x</sub> to HNO<sub>3</sub> transformation rate (percent per hour), [O<sub>3</sub>] is the background ozone concentration (parts per million),  $S$  is the atmospheric stability index, according to the Pasquill–Gifford–Turner classification (Gifford 1976) ranging from 2 (moderate unstable) to 6 (moderate stable) and [NO<sub>x</sub>]<sub>m</sub> is the vertically averaged NO<sub>x</sub> concentration (parts per million). The expression of

the vertically averaged concentration ( $C_m$ ) can be obtained integrating expression 1:

$$C_m(x) = \frac{1}{h} \int_{z=0}^{z=h} C(x,z) dz$$

$$= \frac{a \left[ Q_0 x^b + \sum_{i=1}^N (Q_i - Q_{i-1})(x-x_i)^b \right]}{|A_1| k z_0^b u_*} \sum_{j=0}^6 \frac{A_j}{j+1}$$
(5)

During night-time,  $\text{NO}_x$  oxidation to nitric acid and nitrates is believed to be slow due to the absence of the hydroxyl radical. Since these reactions are, in general, less important than daytime oxidation rates, a constant oxidation rate of 2% per hour can be assumed for night-time conditions (Scire et al. 2000).

The air concentrations of  $\text{NO}_2$  ( $C_{\text{NO}_2}$ ) and  $\text{HNO}_3$  ( $C_{\text{HNO}_3}$ ) after the reactions, can be calculated assuming the following pseudo-first-order reactions mechanism (Scire et al. 2000):

$$C_{\text{NO}_2}(x,z) = C_{\text{NO}_x}(x,z) \exp[-k_1 \Delta t / 100]$$
(6)

$$C_{\text{HNO}_3}(x,z) = C_{\text{NO}_x}(x,z) [1 - \exp(-k_2 \Delta t / 100)]$$
(7)

where  $C_{\text{NO}_x}(x,z)$  is the initial concentration of  $\text{NO}_x$  (parts per million; given by Eq. 1) and  $\Delta t$  is the model time step (=1 h).

### 3.1.1 Wet Deposition Parameterization

Assuming the plume of contaminants is below a raining cloud, the wet deposition flux of air pollutants,  $F_w$  (mass per area per time), can be calculated by (Seinfeld and Pandis 1998):

$$F_w(x) = \int_0^h \Lambda C(x,z) dz$$
(8)

where  $\Lambda$  is the scavenging ratio (per second; this nomenclature is consistent with the CALPUFF User’s Guide). Wet deposition is a complex process that depends on pollutant properties and the drop size distribution. However, an estimation of  $F_w$  can be obtained after some simplified assumptions. Assum-

ing that  $\Lambda$  does not vary with height and replacing the vertical integral of  $C(x,z)$  using Eq. 5, Eq. 8 can be expressed as:

$$F_w(x) = \Lambda \int_0^h C(x,z) dz = \Lambda h(x) C_m(x)$$
(9)

Considering the expression of the scavenging ratio parameterized in function of the rain rate ( $p_0$ ) and a scavenging coefficient ( $\lambda$ ) which depends on the gaseous specie (Maul 1980; Scire et al. 2000),  $F_w$  can be estimated as:

$$F_w(x) = \lambda(p_0/p_1)h(x)C_m(x)$$
(10)

where  $p_1$  is a reference value (=1 mm h<sup>-1</sup>). In this way,  $F_w$  is evaluated as the product of a scavenging coefficient, the precipitation rate, the vertical extension of the plume below the cloud and the averaged air pollutant concentration which is similar to the methodology included in well used atmospheric dispersion–deposition models (Scire et al. 2000; Wesely et al. 2002; US EPA 2004).

The scavenging coefficient is considered zero for  $\text{NO}_2$  and 6.0E-05 s<sup>-1</sup> for  $\text{HNO}_3$  (Scire et al. 2000). The zero scavenging coefficient for nitrogen dioxide results from its low solubility in water. The uptake of  $\text{NO}_2$  by raindrops occurs through reactions which are too slow under ambient conditions and hence, the removal of  $\text{NO}_2$  by precipitation results negligible (Lee and Schwartz 1981).

The removal rate of air pollutant concentration ( $dC/dt$ ) due to rain scavenging is given by:

$$\frac{dC}{dt} = -\Lambda C$$
(11)

In this way, ground-level air pollutant concentration ( $C'$ ) after the wet removal process, can be obtained integrating Eq. 11 as

$$C'(x, 0) = C(x, 0) \exp(-\Lambda \Delta t)$$
(12)

where  $C(x,0)$  is ground-level air pollutant concentration before the wet removal process.

### 3.1.2 Dry Deposition Parameterization

Considering that dry deposition process affects  $C'(x,0)$ , dry deposition flux is estimated as:

$$F_d = v_d C'(x, 0) \quad (13)$$

where  $v_d$  is the dry deposition velocity (meter per second) of the pollutant.

Dry deposition velocities are estimated considering the resistance method (Seinfeld and Pandis 1998). This method assumes that the transport of gaseous pollutants to the surface is governed by three resistances in series: the aerodynamic resistance,  $r_a$ , the quasi-laminar sub-layer resistance,  $r_d$ , and the surface resistance,  $r_w$  (water surface in this case). Under steady state conditions, the dry deposition velocity for gaseous pollutants can be expressed as follows (Seinfeld and Pandis 1998):

$$v_d = (r_a + r_d + r_w)^{-1} \quad (14)$$

The aerodynamic resistance,  $r_a$ , represents the turbulent transport of the pollutant through the atmospheric surface layer, and can be calculated following the Monin-Obukhov similarity theory, as:

$$r_a = [\ln(z_r/z_0)] - \varphi_H(z_r/L) / k u_* \quad (15)$$

where  $z_r$  is a reference level near the surface (usually 1 m) and  $\varphi_H$  is a stability correction term (Seinfeld and Pandis 1998; Arya 1999). The roughness length ( $z_0$ ) over the water surface is computed as a function of wind speed ( $u$ ) as:

$$z_0 = 2.0E - 06 u^{2.5} \quad (16)$$

where  $u$  is the wind speed (meter per second) at 10 m and  $z_0$  is in meters.

The quasi-laminar sub-layer resistance,  $r_d$ , is related to the transfer of the species in a very thin layer close to the surface, where transport is mainly controlled by molecular processes. The resistance of the quasi-laminar sub-layer is parameterized as (Scire et al. 2000; US EPA 2004):

$$r_d = d_1 Sc^{d_2} / (k u_*) \quad (17)$$

where  $Sc$  is the Schmidt number (ratio between kinematic viscosity of air and molecular diffusivity of modeled gas in air),  $d_1=2$  and  $d_2=2/3$ .

Finally, over the water surface, the transfer of the substance through the interface depends mainly on the solubility and reactivity of the pollutant in water. Hence, the resistance of the water surface,  $r_w$ , is computed in terms of the Henry's Law constant ( $H$ ) and a solubility enhancement factor due to reactivity ( $\alpha_*$ ) as:

$$r_w = H / (\alpha_* d_3 u_*) \quad (18)$$

where  $d_3$  is a constant ( $=4.8E-04$ ). It is considered  $H=3.5$  for  $NO_2$  and  $8.0E-08$  for  $HNO_3$  and  $\alpha_*=10$  for both species (Scire et al. 2000).

### 3.2 CALPUFF Model

CALPUFF model (Scire et al. 2000) is applied to estimate the dry and wet deposition of nitrogen coming from point source emissions over waters of de la Plata River. CALPUFF is an atmospheric dispersion model recommended by US EPA for characterization of long-range transport. It is a multi-layer, non-steady-state, Lagrangian puff model which can simulate the effect of meteorological conditions on air pollutant concentration. This model represents a continuous plume as a number of discrete packets of pollutant material (puffs). Each puff is free to evolve independently in response to local effects of transport, dispersion, chemical transformation and deposition during particular time intervals. At the end of each time step, the puffs are "frozen" and the pollutant concentration at each receptor is computed as the sum of the contributions of all nearby puffs.

In this application, CALPUFF calculations have been done in screening mode (US EPA 1998) and selecting the slug option. The reason for selecting the screening mode is the lack of enough meteorological information available. Nevertheless, as the terrain is flat and the region of study is over water, concentration and deposition estimates will be reasonably conservative when compared to a CALPUFF modeling with a fully developed wind field. In the slug option, the "puffs" consist of Gaussian packets of pollutant material stretched in the along-wind direction. A slug can be visualized as a group of overlapping circular puffs having very small puff separation distances. The slug option ensures continuity of a simulated plume without the gaps associated with the puff approach. The concentration distribution



estimated under the slug option approaches that of the Gaussian plume result under the appropriate steady-state conditions (Scire et al. 2000).

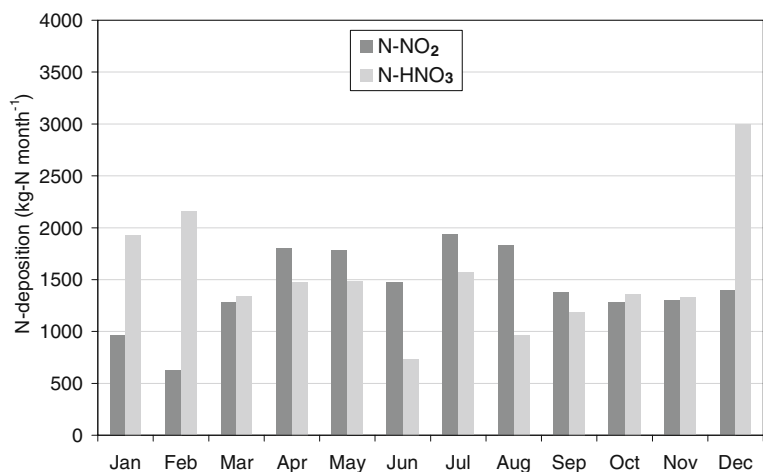
#### 4 Atmospheric N Deposition to de la Plata River

Atmospheric deposition of nitrogen to coastal surface waters of the de la Plata River is estimated applying DAUMOD-RD (v.2) and CALPUFF models to the  $\text{NO}_x$  emitted from area and point sources located in the city of Buenos Aires, respectively. Calculations are performed with a spatial resolution of  $1 \text{ km}^2$  covering  $1,763 \text{ km}^2$  of the river. One year (1999) of hourly surface meteorological information registered at the Domestic Airport of Buenos Aires and sounding data obtained at Ezeiza International Airport (located 30 km southwest of the city) are used. Monthly mean ozone concentrations varying between 30–60 ppb, based on results from campaigns carried out near the coast (Bogo et al. 1999; Mazzeo et al. 2005), have been considered for model calculations. In addition, emission data of the high spatial resolution ( $1 \text{ km}^2$ ) emissions inventory developed for Buenos Aires city (Mazzeo and Venegas 2003) are used. These emission data include hourly values of area source emissions according to a typical diurnal variation. On the other hand, point source emission strengths are reported as mean values for each stack of the thermal power plants. These power plants burn natural gas during most part of the year except for the coldest days in winter (usually no more than 15), when they are compelled to burn gas-oil.

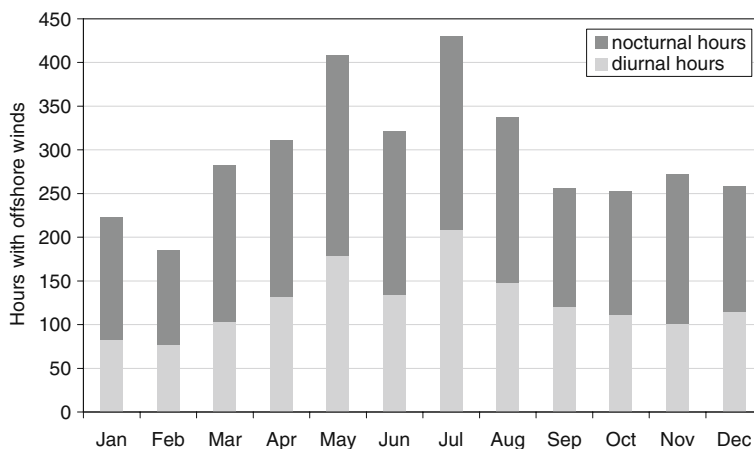
One consideration to take into account is that this modeling approach does not produce 3-dimensional wind fields, so land–sea breezes are not modeled. Breeze circulations over the wide estuary of the river could bring pollutants back to the receptor area. However, the frequency of atmospheric recirculation events over the city is small: 8% in summer, 7% in autumn, 5% in winter and 7% in spring (Venegas and Mazzeo 1999). In this way, it is expected that this modeling limitation will not significantly affect the results.

Figure 3 shows the monthly variation of (dry+wet) deposition of  $\text{N-NO}_2$  and  $\text{N-HNO}_3$  to the river. It is observed that the greatest contribution to total N deposition results from  $\text{N-HNO}_3$  deposition in December. The deposition of  $\text{N-NO}_2$  varies between  $630 \text{ kg-N month}^{-1}$  in February and  $1,934 \text{ kg-N month}^{-1}$  in July. The pattern of this monthly variation is similar to the monthly variation of the number of hours with offshore wind, as can be seen in Fig. 4. The frequencies of winds towards the river are greater from May to August (most winter) than during summer months (December, January and February). Monthly total (dry+wet) deposition of  $\text{N-HNO}_3$  varies between  $736 \text{ kg-N month}^{-1}$  in June and  $2,998 \text{ kg-N month}^{-1}$  in December (Fig. 3). In this month the  $\text{N-HNO}_3$  deposition is considerably greater than in other summer months. This is because during December there have been more favorable situations for deposition at diurnal hours (i.e., hours with greater  $\text{NO}_x$  emission and greater  $\text{HNO}_3$  formation) than in the other months of the same season. During December, the number of hours with offshore winds

**Fig. 3** Monthly variation of  $\text{N-NO}_2$  and  $\text{N-HNO}_3$  deposition ( $\text{kg-N month}^{-1}$ ) to de la Plata River



**Fig. 4** Monthly variation of the number of hours with offshore winds



in the diurnal period (taken as 8:00 A.M.–7:00 P.M.) is 37% greater than in January and 48% greater than in February (see Fig. 4). Total N ( $N-NO_2+N-HNO_3$ ) deposition varies between 2,214 kg-N month<sup>-1</sup> in June and 4,399 kg-N month<sup>-1</sup> in December.

Results on Fig. 5 show that both total dry ( $N-NO_2+N-HNO_3$ ) and wet ( $N-HNO_3$ ) deposition (kg-N month<sup>-1</sup>) to de la Plata River have a marked monthly variation. Nitrogen ( $N-NO_2+N-HNO_3$ ) dry deposition varies between 1,628 kg-N month<sup>-1</sup> in February and 3,799 kg-N month<sup>-1</sup> in December. These results show that monthly variation of dry deposition is mainly related to the occurrence of offshore winds during the month (Fig. 4).

On the other hand, wet deposition of nitrogen varies from 1 kg-N month<sup>-1</sup> in June to 1,162 kg-N month<sup>-1</sup> in February. Nitrogen ( $N-HNO_3$ ) wet deposition is generally small, compared to the dry

contribution (Fig. 5). This is mainly due to the fact that a very few hours with offshore winds showed rain events. Combining values displayed in Figs. 4 and 6, it results that the number of hours with offshore wind and precipitation event is very small for all months. Rainy offshore wind conditions vary between 1.2% of offshore wind hours in September and 8.9% in January. Also, the greater formation of  $HNO_3$  during summer leads to a greater wet deposition during this season. This significant variation is also due to the variation of monthly precipitation as can be seen in Fig. 7. Monthly precipitation with offshore winds varied from 1.5 mm in September to 62.2 mm in March.

As mentioned above, the time of the day in which favorable situations for deposition occur is another important factor. As shown in Fig. 6, among the summer months (December, January and February),

**Fig. 5** Monthly variation of total N wet ( $N-HNO_3$ ) and dry ( $N-NO_2+N-HNO_3$ ) deposition (kg-N month<sup>-1</sup>) to de la Plata River

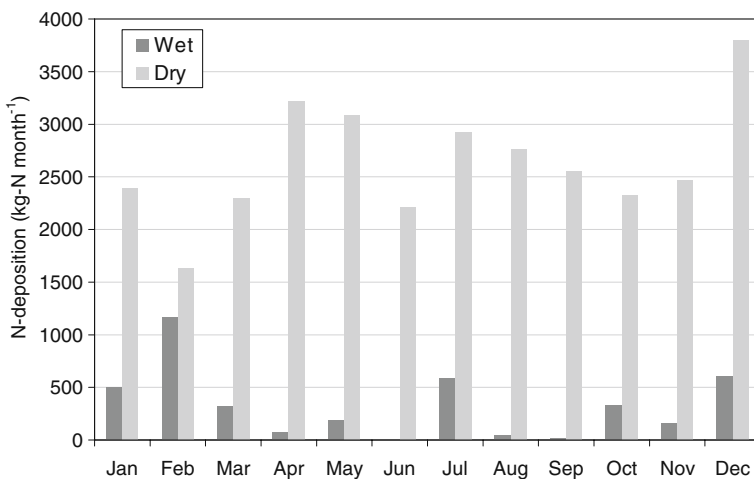
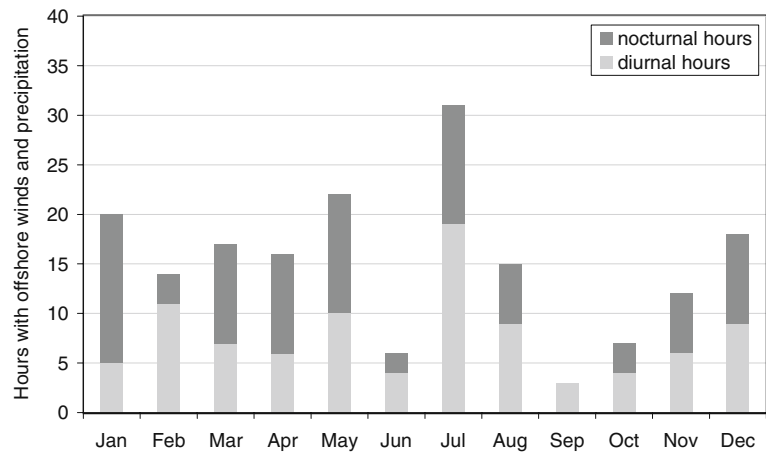




**Fig. 6** Monthly variation of the number of hours with offshore winds with precipitation



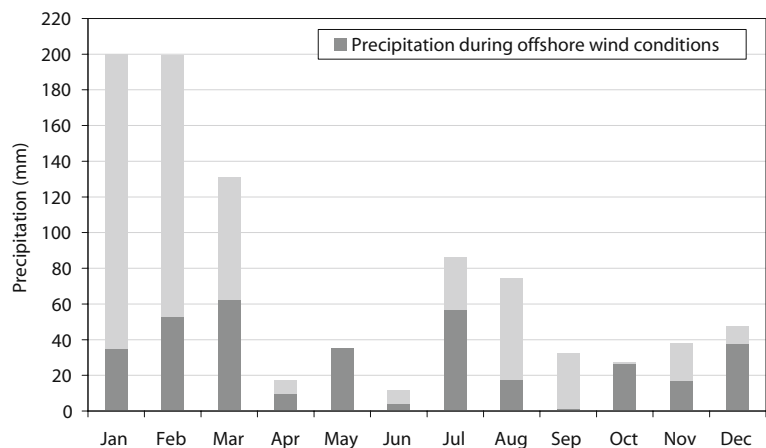
February presents the greatest number of situations with offshore winds and precipitation during diurnal hours. In particular, in this month wet deposition of nitric acid exceeds its dry deposition. In the same way, the particularly high wet deposition value obtained in July (Fig. 5) may be explained by the great number of conditions with winds towards the river and precipitation during diurnal hours, compared to other months of winter (June, July and August). On the other hand, the lowest number of hours with offshore winds and precipitation registered in June and the small  $\text{HNO}_3$  formation rates (expected during winter time), result in the extremely low ( $\sim 1$  kg-N month<sup>-1</sup>) wet deposition value obtained for this month.

Finally, the obtained total N annual deposition to 1,763 km<sup>2</sup> of the river is 35,600 kg-N year<sup>-1</sup> (31,638 kg-N year<sup>-1</sup> dry and 3,962 kg-N year<sup>-1</sup> wet deposited). Comparing with the results obtained in a

previous work (Pineda Rojas and Venegas 2008) in which only dry deposition to the river has been estimated, it can be concluded that the inclusion of wet deposition processes in the DAUMOD-RD (v.2) model has lead to an increase of 12.1% in total N deposition, while N dry deposition decreased only 0.4% due to the fact that rain scavenge reduces the air concentration of the nitric acid near the water surface.

At present, nitrogen discharges from the main tributaries and sewage from the Metropolitan Area of Buenos Aires (MABA: Buenos Aires City+Greater Buenos Aires) to the river are large. For example, according to Villar and Bonetto (2000) and Villar et al. (2002), the nitrogen loading from the main tributaries is 440 ton-N day<sup>-1</sup> for nitrate and 60 ton-N day<sup>-1</sup> for ammonia species. Menendez et al. (2002) estimated the nitrate loading from MABA to be about 60 ton-N day<sup>-1</sup>, while that from the main tributaries is 400 ton-N day<sup>-1</sup>. Ammonia discharge obtained by

**Fig. 7** Monthly variation of precipitation (mm) and precipitation occurred during offshore wind conditions (mm)



these authors is 180 ton-N day<sup>-1</sup> from the Metropolitan Area of Buenos Aires and 100 ton-N day<sup>-1</sup> from the main rivers (Paraná and Uruguay). According to a recent report (FREPLATA 2004), the ammonia discharge from the coast of the MABA to the river is 78 ton-N day<sup>-1</sup>. Despite the discrepancies between these estimations, the contribution of the atmospheric deposition of oxidized nitrogen (as N-NO<sub>2</sub>+N-HNO<sub>3</sub>) coming from Buenos Aires city emissions to total inorganic N loading to the river appears to be very low (<1%).

Horizontal distribution of annual dry N deposition is shown in Fig. 8. A strong coastal gradient with a maximum value of 129 kg-N km<sup>-2</sup> year<sup>-1</sup> in the first coastal square kilometer has been obtained. At 4 km from the coast, the dry deposition values are approximately half the maximum coastal values. Greater deposition flux values are obtained in the region located N-NE from the city, as a result of wind frequencies from the sector SE→SW. Figure 9 shows the annual wind rose obtained from hourly meteorological data. Annually wind directions from the city towards the river (SE→NW) occur 40.5% of the time.

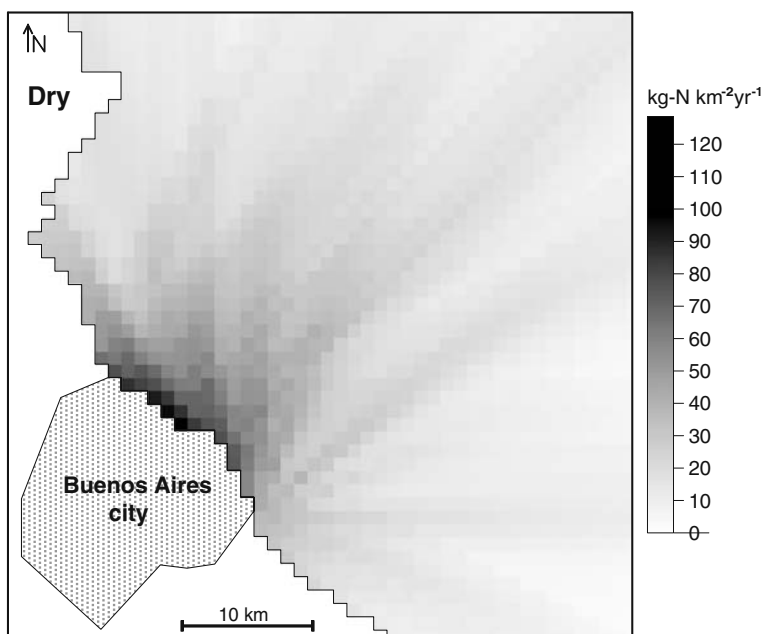
Figure 10 shows the horizontal distribution of annual N wet deposition. This distribution is quite different from that of the dry case. The maximum wet deposition flux is 8.6 kg-N km<sup>-2</sup> year<sup>-1</sup> and it occurs in front of the coast of Buenos Aires city. Moreover,

greater values are obtained in a narrow region parallel to the coast to the north of the city, coincident with the direction of greater superposition of the pollutant plumes coming from the stacks (see Fig. 1). Wet deposition flux shows a secondary maximum of 4.5 kg-N km<sup>-2</sup> year<sup>-1</sup> at ~27 km in the NNE direction.

Results of total N deposition are plotted in Fig. 11. The maximum value (137.1 kg-N km<sup>-2</sup> year<sup>-1</sup>) is obtained in the first square kilometer in front of the Domestic Airport. Beyond 10 km from the coast, total deposition of nitrogen is lower than ~40 kg-N km<sup>-2</sup> year<sup>-1</sup> in all directions. Figure 11 shows a similar pattern than that of N dry deposition due to the low contribution of wet deposition. However, according to the different patterns obtained in dry and wet horizontal distributions, their relative contributions to total N deposition vary spatially. Figure 12 shows the horizontal distribution of the relative (%) contribution of wet deposition to total (wet+dry) N deposition. The contribution of wet deposition in each receptor varies from 4% to 23%, being lower than 10% within the first 10 km from the coast.

Unfortunately, at present there are not available data of measured wet deposition rates in the area of study. Studies of rainfall monitoring data over the city of Buenos Aires have been focused on the characterization of its pH and conductivity (Tafari et al. 1987), reporting that rainfall data in the city showed a pH

**Fig. 8** Horizontal distribution of total N (N-NO<sub>2</sub>+N-HNO<sub>3</sub>) dry deposition (kg-N km<sup>-2</sup> year<sup>-1</sup>) to de la Plata River



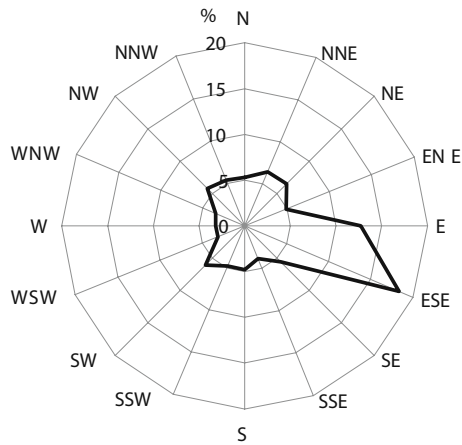


**Fig. 9** Wind rose (direction wind is blowing from) for year 1999

varying between 5.2 and 6.0. For this reason, it is not possible to compare the results obtained in this work with measured wet deposition rates in Buenos Aires. However, a comparison of these results with nitrogen deposition fluxes to coastal waters at other places of the world is included.

Nitrogen deposition fluxes obtained for other coastal sites of the world may vary considerably according to the environmental conditions of the region and the distance to the sources of atmospheric nitrogen ( $\text{NO}_x$

and  $\text{NH}_3$ ). For example, Poor et al. (2001) estimated that the mean N ( $\text{N} - \text{HNO}_3 + \text{N} - \text{NO}_3^-$ ) deposition to Tampa Bay is  $307 \text{ kg-N km}^{-2} \text{ year}^{-1}$ , from which 56% is given by wet deposition. Hertel et al. (2002) obtained that the emissions of  $\text{NO}_x$  lead to an atmospheric N deposition to waters of the North Sea in front of the coasts of different countries between  $500\text{--}900 \text{ kg-N km}^{-2} \text{ year}^{-1}$ , with a wet contribution of more than 80%. According to Gao (2002), total N (as nitrate) deposition to Barnegat Bay (USA) is  $460 \text{ kg-N km}^{-2} \text{ year}^{-1}$ , with a wet contribution of near 88%. Moreover, Carstensen et al. (2005) evaluated the fluxes of total inorganic nitrogen (oxidized and reduced) to the Kattegat, obtaining a mean N deposition value of  $1,020 \text{ kg-N km}^{-2} \text{ year}^{-1}$ , with a relative contribution of wet deposition of 79%. On the other hand, background total inorganic N deposition estimated for the region of de la Plata River using a global transport-chemistry model and considering both natural and anthropogenic N sources is  $600 \text{ kg-N km}^{-2} \text{ year}^{-1}$  (Galloway et al. 2004). Taking into account that this work studies the deposition of N ( $\text{N} - \text{NO}_2 + \text{N} - \text{HNO}_3$ ) and considers the  $\text{NO}_x$  emitted only in the city of Buenos Aires, the maximum coastal N deposition value obtained in this work (up to  $137 \text{ kg-N km}^{-2} \text{ year}^{-1}$ ) is consistently lower than background deposition values.

**Fig. 10** Horizontal distribution of N ( $\text{N} - \text{HNO}_3$ ) wet deposition ( $\text{kg-N km}^{-2} \text{ year}^{-1}$ ) to de la Plata River

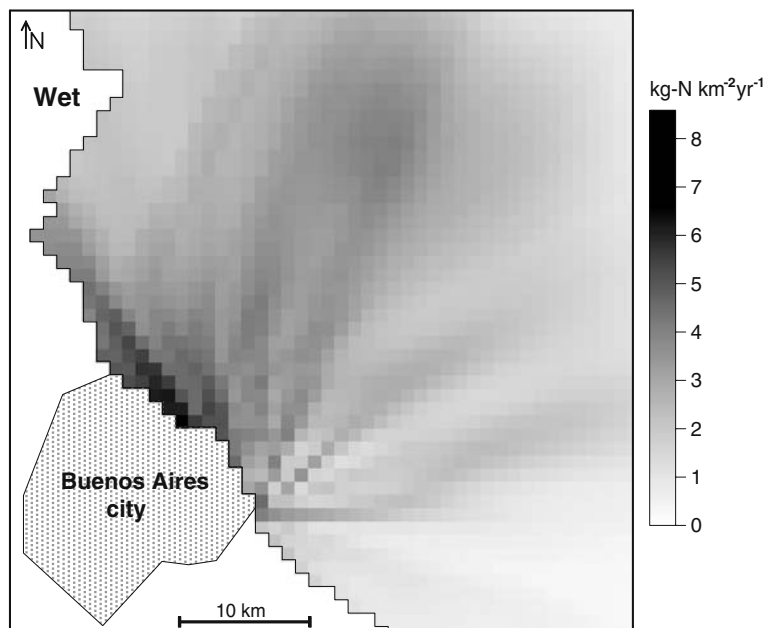
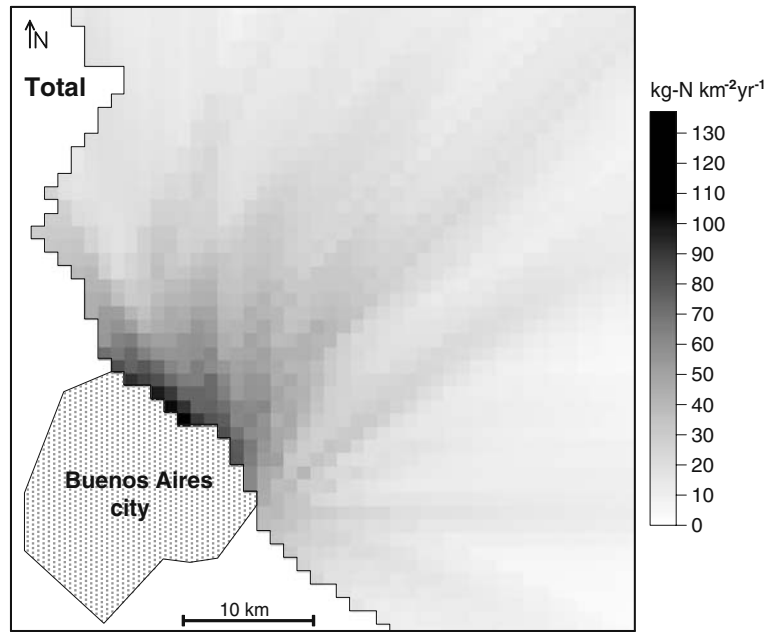


**Fig. 11** Horizontal distribution of total N ( $N-NO_2+N-HNO_3$ ) deposition ( $kg-N\ km^{-2}\ year^{-1}$ ) to de la Plata River

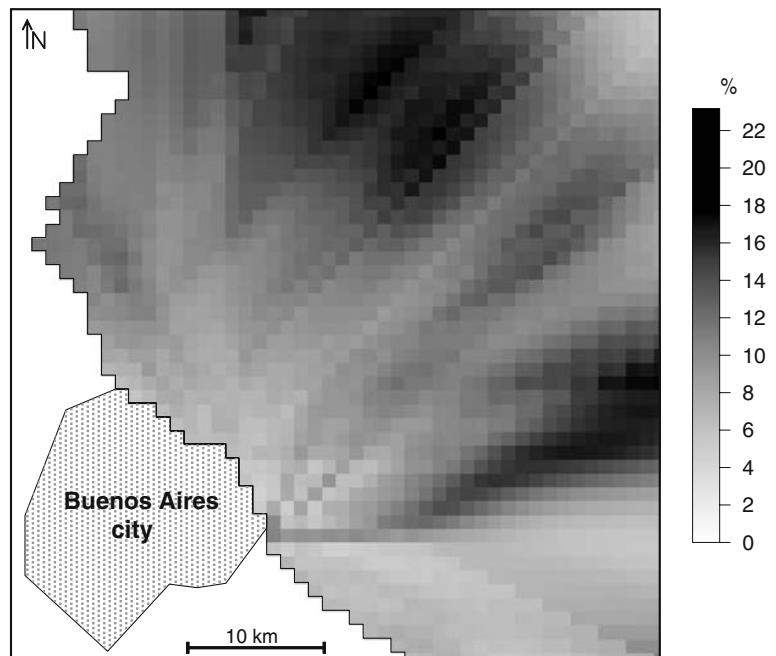


## 5 Conclusions

The first estimation of wet and dry deposition of atmospheric nitrogen to surface waters of de la Plata River in front of Buenos Aires city, are presented. DAUMOD-RD (v.2) and CALPUFF models have been applied to  $NO_x$  emissions from area and point

sources located in the city of Buenos Aires. Total annual N ( $N-NO_2+N-HNO_3$ ) deposition obtained over  $1,763\ km^2$  of the river is  $35,600\ kg-N\ year^{-1}$ . The contribution of  $HNO_3$  wet deposition to this value is 11%, while dry deposition of  $NO_2$  and  $HNO_3$  contribute with 48% and 41%, respectively. The low contribution of wet deposition to annual N deposition,

**Fig. 12** Horizontal distribution of wet deposition contribution (%) to total N deposition to de la Plata River



results from the very few cases (5%) of rain events during offshore wind conditions. Hence, it is possible to conclude that the annual transfer of N from the atmosphere to the waters of de la Plata River occurs mainly through dry deposition. However, the contribution of wet deposition may be important during short time periods. Wet deposition of nitrogen presents a strong monthly variation which is related to the variation of monthly precipitation occurred during offshore wind conditions and the occurrence of these situations during diurnal hours.

Monthly dry deposition varies strongly with the number of hours with winds towards the river and with the time of the year given that in summer months, the greater photochemical activity of the atmosphere favors the conversion of NO<sub>2</sub> to HNO<sub>3</sub> whose dry deposition velocity is greater than that of NO<sub>2</sub>.

The total N deposition horizontal distribution shows a strong coastal gradient with a maximum of 137.1 kg-N km<sup>-2</sup> year<sup>-1</sup> near the shoreline and values 50% lower at 4 km of distance from the coast. Relative contribution of wet deposition in each receptor varies between 4% and 23%, being greater far from the coast.

**Acknowledgements** This study has been partially supported by Projects UBACyT X060 and CONICET-PIP 6169. The authors wish to thank the National Meteorological Service of Argentina for supplying meteorological data used in this study.

## References

- Arya, S. P. (1999). *Air pollution meteorology and dispersion*. Oxford University Press. pp. 310.
- Atkinson, R. (2000). Atmospheric chemistry of VOCs and NO<sub>x</sub>. *Atmospheric Environment*, 34, 2063–2101.
- Atkinson, R., Lloyd, A. C., & Wings, L. (1982). An updated chemical mechanism for hydrocarbon/NO<sub>x</sub>/SO<sub>2</sub> photooxidations suitable for inclusion in atmospheric simulation models. *Atmospheric Environment*, 16(6), 1341–1355.
- Bartram, J., Carmichael, W. W., Chorus, I., Jones, G. & Skulberg, O. M. (1999). Toxic Cyanobacteria in Water: A guide to their public health consequences, monitoring and management. World Health Organization. Retrieved December 12, 2007, from [http://whqlibdoc.who.int/publications/1999/0419239308\\_eng.pdf](http://whqlibdoc.who.int/publications/1999/0419239308_eng.pdf).
- Bogo, H., Negri, R. M., & San Román, E. (1999). Continuous measurement of gaseous pollutants in Buenos Aires City. *Atmospheric Environment*, 33, 2587–2598.
- Carstensen, J., Frohn, L. M., Hasager, C. B., & Gustafsson, B. G. (2005). Summer algal blooms in a coastal ecosystem: the role of atmospheric deposition versus entrainment fluxes. *Estuarine, Coastal and Shelf Science*, 62, 595–608.
- FREPLATA. (2004). Análisis Diagnóstico Transfronterizo del Río de la Plata y su Frente Marítimo. Documento Técnico. Proyecto Protección Ambiental del Río de la Plata y su Frente Marítimo. Proyecto PNUD/GEF/RLA/99/G31 (in Spanish).
- Galloway, J. N., Dentener, F. J., Capone, D. G., Boyer, E. W., Howarth, R. W., Seitzinger, S. P., et al. (2004). Nitrogen cycles: past, present, and future. *Biogeochemistry*, 70, 153–226.
- Gao, Y. (2002). Atmospheric nitrogen deposition to Barnegat Bay. *Atmospheric Environment*, 36, 5783–5794.
- Garban, B., Motelay-Massei, A., Blanchoud, H., & Ollivon, D. (2004). A single law to describe atmospheric nitrogen bulk deposition versus rainfall amount: inputs at the seine river watershed scale. *Water, Air, and Soil Pollution*, 155, 339–354.
- Gifford, F. A. (1976). Turbulent diffusion typing schemes: a review. *Nuclear Safety*, 17(1), 25–43.
- Hertel, O., Ambelas Skjøth, C., Frohn, L. M., Vignati, E., Frydendall, J., de Leeuw, G., et al. (2002). Assessment on the atmospheric nitrogen and sulphur inputs into the North Sea using a Lagrangian model. *Physics and Chemistry of the Earth*, 27, 1507–1515.
- Imboden, A., Christoforou, S., & Salmon, L. G. (2003). Determination of atmospheric nitrogen input to Lake Greenwood, South Carolina: Part 2 – gaseous measurements and modeling. *Journal of Air and Waste Management Association*, 53, 1499–1508.
- Jickells, T. D. (2002). Emissions from the oceans to the atmosphere, deposition from the atmosphere to the oceans and the interactions between them. In W. Steffen, J. Jäger, D. J. Carson, & C. Bradshaw (Eds.) *Challenger of the changing earth. Proceedings of the global change open science conference*. Amsterdam, The Netherlands: Springer.
- Khoder, M. I. (2002). Atmospheric conversion of sulfur dioxide to particulate sulfate and nitrogen dioxide to particulate nitrate and gaseous nitric acid in an urban area. *Chemosphere*, 49, 675–684.
- Lee, Y., & Schwartz, S. E. (1981). Evaluation of the rate of uptake of nitrogen dioxide by atmospheric and surface liquid water. *Journal of Geophysical Research*, 86(C12), 11971–11983.
- Luo, Y., Yang, X., Carley, R. J., & Perkins, C. (2002). Atmospheric deposition of nitrogen along the Connecticut coastline of Long Island Sound: a decade of measurements. *Atmospheric Environment*, 36, 4517–4528.
- Maul, P. R. (1980). Atmospheric transport of sulfur compound pollutants. Central Electricity Generating Bureau MID/SSD/80/0026/R. Nottingham, England.
- Mazzeo, N. A., & Venegas, L. E. (1991). Air pollution model for an urban area. *Atmospheric Research*, 26, 165–179.
- Mazzeo, N. A., & Venegas, L. E. (2003). Carbon monoxide and nitrogen oxides emission inventory for Buenos Aires City (Argentina). In R. S. Sokhi, & J. Brechler (Eds.) *Fourth international conference on urban air quality – Measurement, modelling and management* (pp. 159–162). Czech Republic: Prague.
- Mazzeo, N. A., & Venegas, L. E. (2004). Some aspects of air pollution in Buenos Aires. *International Journal of Environment and Pollution*, 22(4), 365–379.
- Mazzeo, N. A., Venegas, L. E., & Choren, H. (2005). Analysis of NO, NO<sub>2</sub>, O<sub>3</sub> and NO<sub>x</sub> concentrations measured at a green area of Buenos Aires City during wintertime. *Atmospheric Environment*, 39, 3055–3068.

- Menendez, A. N., Jaime, P., & Natale, O. E. (2002). Nutrients balance in the Río de la Plata River using mathematical modeling. *5th International Conference Hydroinformatics*, Cardiff, UK.
- Nagy, G. J. (2000). Dissolved inorganic NP budget for the frontal zone of the Río de la Plata system. Estuarine systems of the South American region: C, N, P fluxes 2000. In V. Dupra, S. V. Smith, J. I. Marshall Crossland, & C. J. Crossland (Eds.) *Loicz reports and studies 15* (pp. 40–43). The Netherlands: Texel.
- Nagy, G. J., Gómez-Erache, M., López, C. H., & Perdomo, A. C. (2002). Distribution patterns of nutrients and symptoms of eutrophication in the Río de la Plata river estuary system. *Hydrobiologia*, 475/76, 125–139.
- Pineda Rojas, A. L., & Venegas, L. E. (2008). Estimation of dry deposition of atmospheric nitrogen to coastal waters of de la Plata River in front of Buenos Aires city. *International Journal of Environment and Pollution* (in press).
- Pizarro, M. J., & Orlando, A. M. (1985). Distribución de fósforo, nitrógeno y silicio disuelto en el Río de la Plata. Servicio de Hidrografía Naval. Secretaría Marina. *Publicación, H-625*, 1–57.
- Poor, N., Pribble, R., & Greening, H. (2001). Direct wet and dry deposition of ammonia, nitric acid, ammonium and nitrate to the Tampa Bay Estuary, FL, USA. *Atmospheric Environment*, 35, 3947–3955.
- Pryor, S. C., Barthelmie, R. J., Schoof, J. T., Sørensen, L. L., & Erickson III., D. J. (2001). Implications of heterogeneous chemistry of nitric acid for nitrogen deposition to marine ecosystems: observations and modelling. *Water, Air, and Soil Pollution: Focus*, 1, 99–107.
- Pryor, S. C., & Sørensen, L. L. (2002). Dry deposition of reactive nitrogen to marine environments: recent advances and remaining uncertainties. *Marine Pollution*, 44, 1336–1340.
- Scire, J. S., Lurmann, F. W., Bass, A., & Hanna, S. R. (1984). Development of the MESOPUFF II dispersion model. Environmental Research & Technology, Inc., EPA-600/3-84-057, pp. 91.
- Scire, J. S., Strimaitis, D. G. & Yamartino, R. J. (2000). A user's guide for the CALPUFF dispersion model. Earth Tech Inc., Concord, MA, pp. 521.
- Seinfeld, J. H., & Pandis, S. N. (1998). Atmospheric chemistry and physics of air pollution p. 1326. New York: John Wiley & Sons.
- Tafari, V., Medrano, V., & Achaval, E. M. (1987). Caracterización química de la lluvia en la Ciudad de Buenos Aires. *Anales II Congreso Interamericano de Meteorología*. Buenos Aires. 16.4.1–16.4.4. (in Spanish).
- US EPA. (1998). Analyses of the CALMET/CALPUFF modelling system in a screening mode. United States Environmental Protection Agency. EPA-454/R-98-010, pp. 56.
- US EPA. (2004). AERMOD Deposition Algorithms – Science Document (Revised Draft). Retrieved November 10, 2007, from [www.epa.gov/ttn/scram/](http://www.epa.gov/ttn/scram/).
- Venegas, L. E., & Mazzeo, N. A. (1999). Atmospheric stagnation, recirculation and ventilation potential of several sites in Argentina. *Atmospheric Research*, 52, 43–57.
- Venegas, L. E., & Mazzeo, N. A. (2002). An evaluation of DAUMOD model in estimating urban background concentrations. *International Journal on Water, Air and Soil Pollution: Focus*, 2(5–6), 433–443.
- Venegas, L. E., & Mazzeo, N. A. (2006). Modelling of urban background pollution in Buenos Aires City (Argentina). *Environmental Modelling & Software*, 21, 577–586.
- Villar, C. A., & Bonetto, C. (2000). Chemistry and nutrient concentrations of the lower Paraná river and its floodplain marshes during extreme flooding. *Archiv für Hydrobiologie*, 148(3), 461–479.
- Villar, C. A., Stripeikis, J., d'Huicque, L., Tudino, M., & Bonetto, C. (2002). Concentration and transport of particulate nutrients and metals in the lower Paraná river during extreme flooding. *Archiv für Hydrobiologie*, 153 (22), 273–286.
- Wesely, M. L., Doskey, P. V., & Shannon, J. D. (2002). Deposition Parameterizations for the Industrial Source Complex (ISC3) Model, Argonne National Laboratory, Argonne, Illinois 60439.
- Whitall, D., Hendrickson, B., & Paerl, H. (2003). Importance of atmospherically deposited nitrogen to the annual nitrogen budget of the Neuse River estuary, North Carolina. *Environment International*, 29, 393–399.